DIURNAL ANISOTROPIES IN THE COSMIC RAY MUON INTENSITY NEAR SEA LEVEL

A

Thesis

Submitted to

Faculty of Graduate Studies, University of Manitoba,

in partial fulfillment of the requirements for the

degree of Master of Science

by

S. M. Flackman

Winnipeg, Manitoba

September, 1971

ABSTRACT

A meson telescope array located at the University of Manitoba, Winnipeg, Manitoba (geographic longitude 97.2° west and geographic latitude 49.9° north, altitude 236 metres) was used to collect data on muon intensity for a two year period, March 18, 1969 to March 17, 1971. This period occurred shortly after a maximum in the cycle of solar activity. The data were analyzed for the presence of diurnal time variations in solar and sidereal time. The results were compared with earlier observations made with the same apparatus shortly before the solar maximum.

Solar diurnal and semidiurnal anisotropies having amplitudes and phases in general agreement with the earlier work were found; however slight phase shifts to earlier times were noted. The sidereal results were inconclusive.

ACKNOWLEDGEMENTS

Appreciation is extended to Professor S. Standil for his guidance and support.

The author is indebted to Mr. R. B. Hicks and Dr. R. W. Flint for their many helpful discussions and suggestions. Their constant interest and encouragement is gratefully acknowledged.

The author is also grateful to his wife, Bev, for her assistance and understanding in the preparation of this thesis.

CONTENTS

List of Figures

CHAPTER I

INTRODUCTION

The existence of cosmic rays was stumbled upon at the turn of the century. Experimentalists, studying atmospheric effects (Elster, 1900; Gertel, 1900) and ionization chambers (Wilson, 1900, 1901) were plagued by a hitherto unknown ionizing agent in the air. Wilson speculated on extraterrestrial sources of this keenly penetrating radiation. Subsequently, Hess confirmed its existence to altitudes of 5 kilometres (1911, 1912) and Kolhorster to 9 kilometres (1913). Further progress was slow until the application of new techniques, by Skobeltzyn (1927) with the cloud chamber and Bothe and Kolhorster (1928, 1929) with Geiger-Muller counters, in the late twenties.

Clay's observation of the latitude effect (1927) heralded a new phase in the study of cosmic rays. The latitude effect suggested a geomagnetic influence on the cosmic rays before entering into the terrestrial atmosphere, which further suggested that these primary cosmic rays were charged particles.

The 1930's saw further sophistication in the facilities of study with Rossi's (1930a, 1930b) fast coincidence method of multiple counter discharges and Blackett and Occhialini's (1933) counter controlled expansion of a cloud chamber. These methods, applied to earlier absorption experiments, led to the qualitative observation

that cosmic rays, near sea level, were composed of hard and soft components, designated by their susceptibility to absorption in lead.

By this time cosmic rays had achieved the position of a recognized independent field of physical study, with men such as Fermi, Compton, Euler and Rossi devoting their energies to its study.

The investigation of cosmic rays was mainly of a qualitative nature, with the study of elementary particles discovered in cosmic rays achieving fruition in accelerator experiments after World War II. Those cosmic rays entering the earth's atmosphere from the cosmos were referred to as primary. Upon entering the atmosphere these primary cosmic rays collide with air nuclei with an absorption length of approximately 120 g/cm^2. Because of the relativistic energies of these particles, as high as 10^{21} e V, the products of a collision will continue in the general direction of the initial particle. Waddington (1960) reports the constituents of primary radiation to be 84.9% protons, 12.7% alpha particles and 1.4% heavier nuclei. The interaction of the incoming primary, upon collision with an air nucleus, produces the initial secondary cosmic rays, which are mainly comprised of nucleons, antinucleons, pions (charged and neutral), kaons and hyperons. These products decay into muons, electrons, positions, photons, neutrinos and antineutrinos. The muons result mostly from the decay of the charged pions ($\tau_0^2 = 2.55 \times 10^{-8}$ sec.)

$$\pi^+ \longrightarrow \mu^+ + \nu$$
$$\pi^- \longrightarrow \mu^- + \bar{\nu}$$

whereas the main decay process of the uncharged pion ($\tau_0 = 1.1 \times 10^{-14}$ sec.) is: $\pi^\circ \longrightarrow 2\gamma$

giving photons and, by pair production, electrons and positrons. Secondary cosmic rays near sea level are further subdivided into hard and soft components. The soft component penetrates less than 10 cm. of lead and is associated with electron-photon showers, the hard component penetrates more and consists mainly of muons. Rossi (1948) measured a vertical intensity, beneath 15 cm. of lead at sea level, of 0.83×10^{-2} cm.$^{-2}$ sec.$^{-1}$ sterad^{-1} at a latitude of 50° .

Geomagnetic effects

The realization of the influence of the geomagnetic field on cosmic rays was made by Clay (1927) in his observation of the latitude effect. This pointed to the fact that primary cosmic rays were charged particles, reacting to the influence of the earth's magnetic field. Further, the observation of the east-west asymmetry (Johnson 1933, Rossi 1934) showed these primary charged particles to have a positive sign.

The earth's magnetic field can be approximated by a dipole at the centre of the earth. The predominant influences of this geomagnetic field on primary cosmic rays are:

i) there exists a cut-off energy for primary particles, under the influence of this magnetic field, below which a particle cannot reach a particular point on the earth's surface.

ii) for particles of a particular energy arriving at given zenith and azimuth angles on the earth's surface, there exists a particular asymptotic direction in space, determined by the particles' energy and the magnetic field, from which these particles can arrive.

Intensity variations

The course of investigations of cosmic radiations has led to the discovery that the directional distribution of the primary radiation is essentially isotropic. This suggests that the cosmic particles are stored in spatial regions for long periods and during this storage they are sufficiently stirred so as to mask any directional anisotropy arising from their points of origin. However, in the study of the primary and secondary particles, small directional anisotropies and time variations do appear. These temporal variations are classed into those of a periodic nature and those which have no apparent periodicity. There are two sources of non-periodic variations: sudden and large atmospheric temperature and pressure changes, and extra-terrestrial effects. The former affect the production and interaction level of secondaries in the atmosphere which is reflected in the intensity at sea level, while the latter (eg. magnetic storms and solar flares) act directly on the primary flux. The periodic anisotropies manifest themselves in 12 hour (semi-diurnal), 24 hour (diurnal), 27 day, 1 year and 11 year modulations. The magnitudes of the observed anisotropies are dependent both on primary particle energies and solar activity. It has also been suggested that there exists an anisotropy relative to the fixed stars,i.e. a siderral-time variation.

Solar modulation with amplitude of the order of 0.5% was first discovered by Lindholm (1928) and later confirmed by Compton (1932), Hess and Graziadei (1936), Schonland (1937), Lange and Forbush (1948)

and many others. The sidereal variations, if real, are an order of magnitude smaller (Jacklyn, 1965; Peacock et al, 1968; Sekido et al, 1968).

The solar daily variation originates because of the interplanetary magnetic field of the inner solar system, maintained by the radial ejection of the solar wind predominantly in and near the solar equitorial plane. According to Parker (1963), this solar wind of approximately 400 km. sec.$^{-1}$ carries with it a "frozen in" magnetic field. This field has the geometry of an Archimedian spiral due to solar rotation. The field direction crosses the earth's orbit at an angle of approximately 45^{o} west of the earth-sun line.

Periodic variations of the primary intensity, on a solar time base, can be well approximated by first and second harmonic components, the duirnal and semi-duirnal anisotropies. Suggestions of sources of these anisotropies include:

i) azimuthal streaming, proposed independently by Parker (1964, 1967) and Axford (1965). Cosmic rays partake in the rotation of the interplanetary magnetic field resulting in a free space intensity maximum appearing from 90^{o} east of the earth-sun line. This produces a solar duirnal variation and is now accepted as the major cause of the observed average diurnal variation.

ii) solar absorption of cosmic rays, discussed by Mercer and Wilson (1965) as a removal anisotropy along the interplanetary field direction toward the sun.

iii) cosmic ray scattering at magnetic irregularities along the solar field directions either toward or away from the sun as dis-

cussed by Sarabhai and Subramanian (1966) and Patel et al. (1968). Averaging over long periods should cancel these fluctuations since they may appear from either of two directions on a given day.

iv) anisotropy maxima from directions perpendicular to the solar field as demonstrated by Ables et al. (1966) and postulated by Subramanian and Sarabhai (1967) and Lietti and Quenby (1968). This process contributes to the semi-diurnal anisotropy and arises from the cosmic ray density gradient perpendicular to the ecliptic plane.

Sidereal anisotropies might be expected to arise as a result of the distribution of sources within the galaxy. However, because of the randomizing of particle directions in the galactic magnetic field, one would expect to observe these anisotropies only at the highest energies. Swinson (1969, 1970, 1971) proposes a model to account for observed sidereal variations due to cooperative effects of the interplanetary magnetic field and the radial heliocentric cosmic ray density gradient.

This thesis will consider the first and second harmonics of duirnal variations in both solar and sidereal time bases. Two years of data, from March 13, 1969 to March 17, 1971, collected from the meson telescope array at Winnipeg (geographic longitude 97.2° west and geographic latitude 49.9° north, altitude 236 metres) is analyzed. This work extends that of Briggs (1969) who has reported similar results for an earlier period of 18 month duration. Briggs' results were obtained just before the solar activity maximum of 1968-1969 and the results reported here pertain to a period just after the above maximum.

CHAPTER II

APPARATUS AND DATA

2.1 Apparatus

The muon telescopes used for the collection of data considered in this thesis are essentially those described by Briggs (1965, 1969). The only change in the apparatus was the adoption of a more efficient and fully automated data collection system. A brief description of the apparatus now follows.

In total, twelve scintillation detectors were used, in various configurations to form two inclined, two narrow angle vertical and two wide angle vertical telescopes. The two inclined telescopes provided viewing directions in the equatorial plane at 15° west and east of south and exhibited a maximum response to secondary radiation resulting from primaries with energies of around 80 G e V. The vertical telescopes had a lower maximum response to primary energies of around 10 G e V.

The twelve scintillation detectors are grouped into an 'eight detector array' (Briggs and Standil, 1966), comprising the inclined and narrow angle vertical telescopes, and a 'megascope', the wide angle vertical telescope. The individual scintillation detectors of the eight detector array are as follows: a light-tight box (1.37 m. x 1.37 m. x 0.36 m.) constructed of 0.02 m. plywood with a reflective

interior; each box contained a N.E. 102 plastic scintillator (approximately 1.3 m. x 1.3 m. x 0.05 m.) placed centrally on the floor of the box with a 5" (0.13 m.) R.C.A. 8055 photomultiplier inserted midway along one side and clear of the internal base by 0.20 m. The physical orientation of the array is given in a three dimensional diagram (Figure 2.1) drawn in perspective but not to scale, omitting the intervening building floors, which act as the telescope absorbers. The detectors are labelled 1 to 8 and will subsequently be referred to by these numbers. The four scintillation detectors comprising the megascope were similar to those described above and were arranged in two pairs, JA, CK and MI, KE, to form the two wide angle telescopes. Between each pair was 0.10 m. of lead absorber. Table 2.1 shows the geometric details of the telescopes monitored (denoted by combining detector designations for detectors connected in coincidence).

Signals from each photomultiplier (rise time 180-200 n sec.) were amplified and fed to an integral discriminator (output = + 5 volt logic pulses 300 n sec. wide) so as to remove most of the unwanted background noise pulses, and then to a coincidence arrangement consisting of simple diode 'AND' gates. Necessary anticoincidence logic eliminated cosmic ray shower events when elements of other telescopes were triggered simultaneously. The telescope rates and the singles rates of the megascope were counted in scalers and the data read out automatically at ten minute intervals (controlled by a timer based on a crystal oscillator) on

Figure 2.1

A three dimensional diagram (not to scale) showing the physical orientation of the eight detector array.

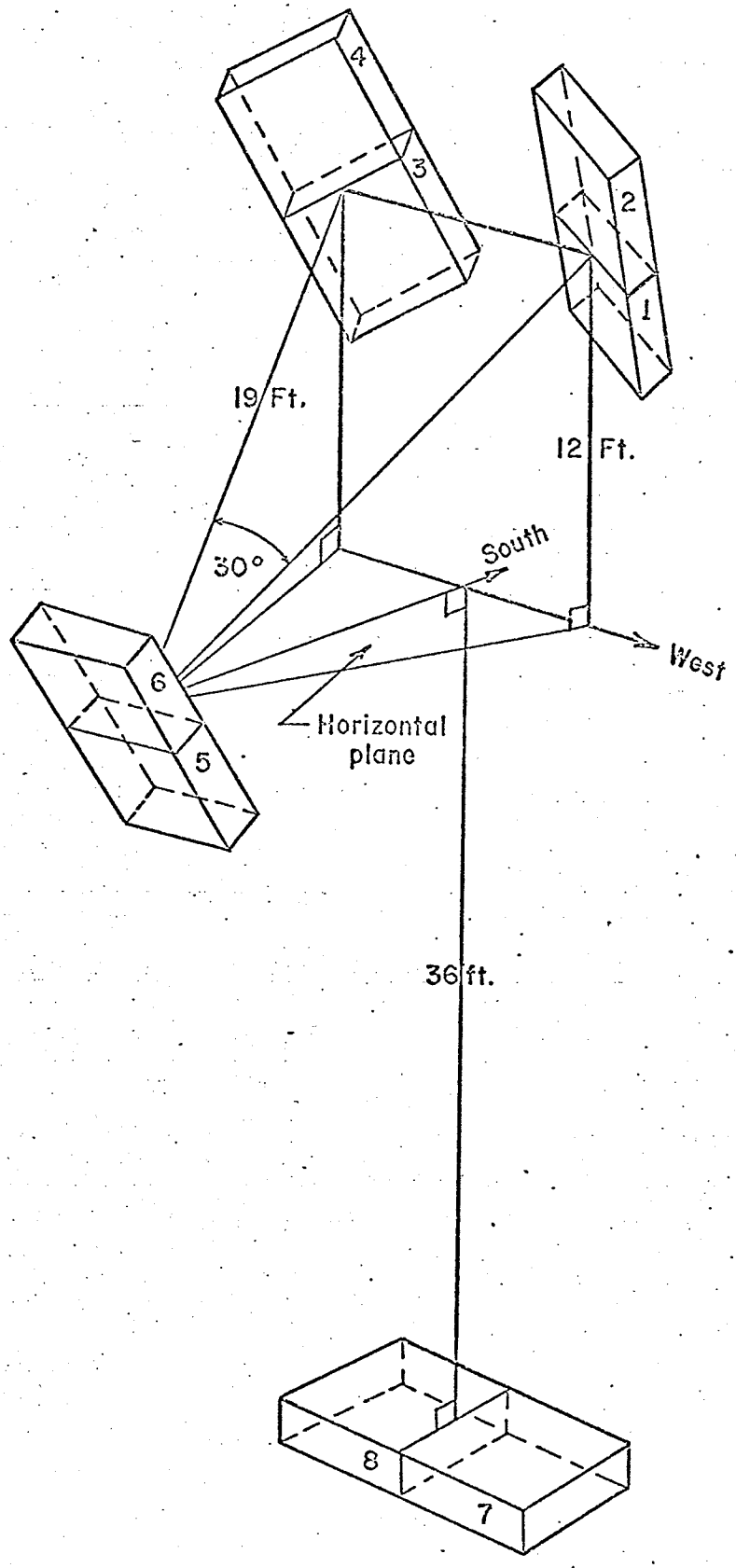
4
3
2
1
1
19 Ft.
12 Ft.
30°
South
West
6
5
Horizontal plane
36 ft.
8
7

TABLE 2.1

GEOMETRIC DETAILS OF MONITORED TELESCOPES

Telescope	Azimuth Angle (east of north)	Zenith Angle	Geometric Factor (cm^2 sterad)	Coincidences/10 min. (approximate)
12-56	199.5°	50.83°	3002	4,900
34-56	160.5°	50.83°	2948	4,800
1234- 7	270.0°	5.85°	342	1,200
1234- 8	90.0°	5.85°	342	1,100
JACK	-	0.0°	3×10^5	80,000
MIKE	-	0.0°	3×10^5	80,000

paper tape by a TALLY tape perforator, model 1505.

2.2 Calibration technique

It was necessary to calibrate the system periodically to set the approximate discriminator levels. The amplified output of each photomultiplier was analyzed as to pulse size while gated by a suitable detector so that the differential spectrum in a given detector was obtained for muons passing through the aperture of the telescope. Some typical spectra are shown in Fig. 2.2. For the eight detector array, the individual discrimination level of each detector was adjusted to correspond to a pulse height equivalent to one-half the muon peak channel number. Because of the better resolution of the muon peaks in the megascope detectors a factor of two-fifths of the muon peak channel number was used here.

2.3 Asymptotic directions of approach

As mentioned in CHAPTER ONE, particles of a given energy arriving at given zenith and azimuth angles at a point on the earth's surface do so from a particular direction in space. This direction is a function of the particle rigidity. For a spectrum of particle energies, this particular direction extends itself into a range of asymptotic directions of approach. These asymptotic directions of approach can be calculated by hypothetically projecting negatively charged particles of chosen rigidities away from the earth as shown in Fig. 2.3 (from McCracken et al, 1962). This was done for the various telescopes utilizing the computer programme formulated by McCracken et al. (1962), modified for the University of Manitoba's

Figure 2.2

Typical muon coincidence peaks used in the calibration technique. Difference in scale of ordinates reflects the difference in gated coincidence rates of the detectors.

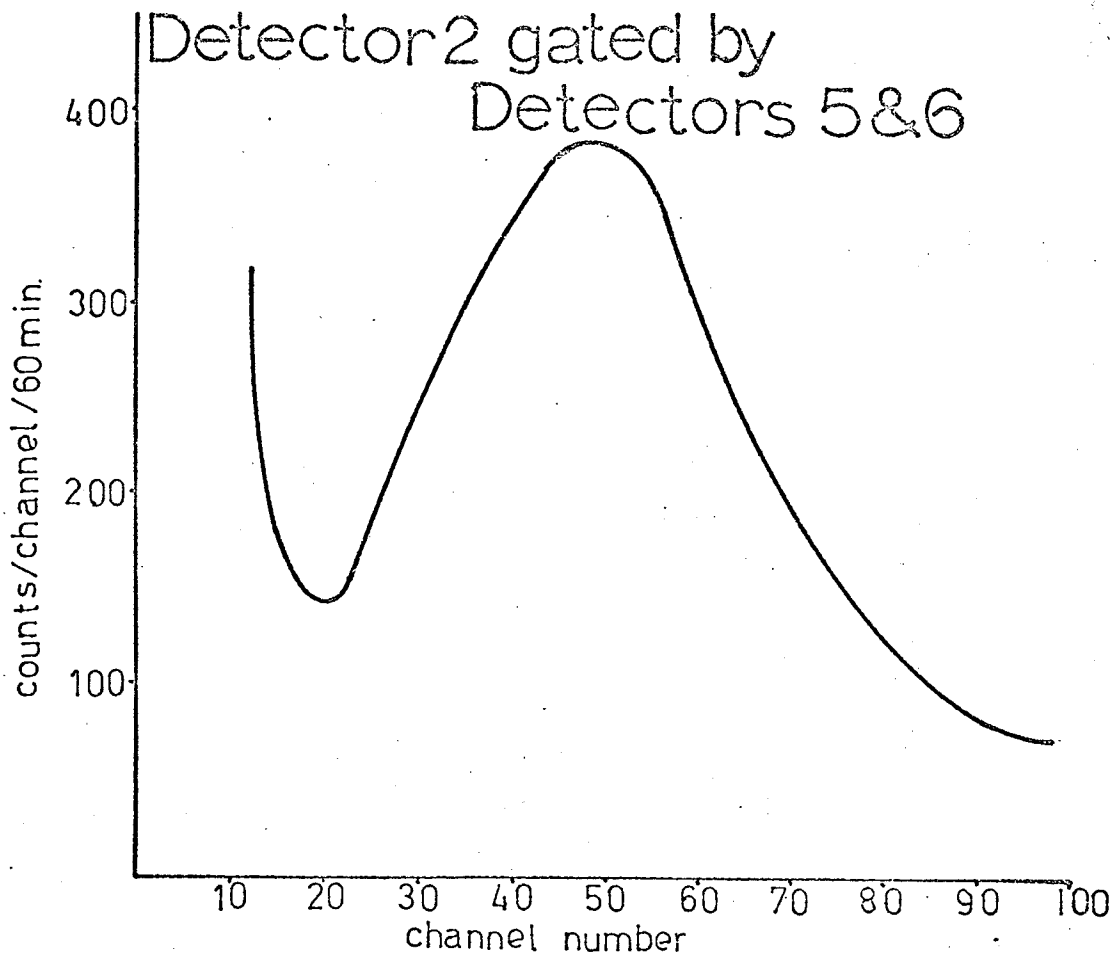
Detector 2 gated by
Detectors 5&6
counts/channel/60 min.
400
300
200
100
10
20
30
40
50
60
70
80
90
100
channel number

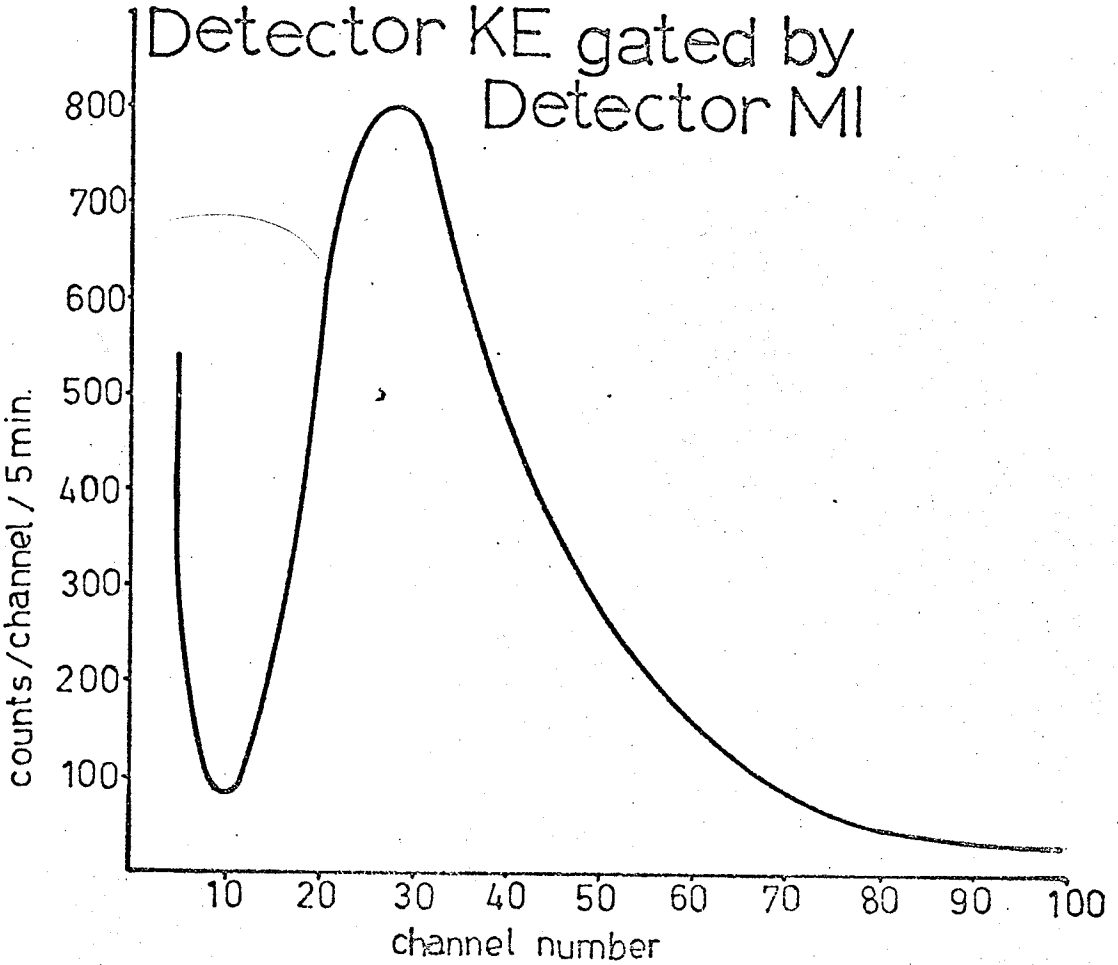
Detector KE gated by
Detector MI
counts/channel/5 min.
800
700
600
500
400
300
200
100
10
20
30
40
50
60
70
80
90
100
channel number

Figure 2.3

A sketch showing the trajectory of either a negatively charged particle receding from the earth or an incoming positively charged primary cosmic ray.

(reproduced from McCracken et al. 1962)

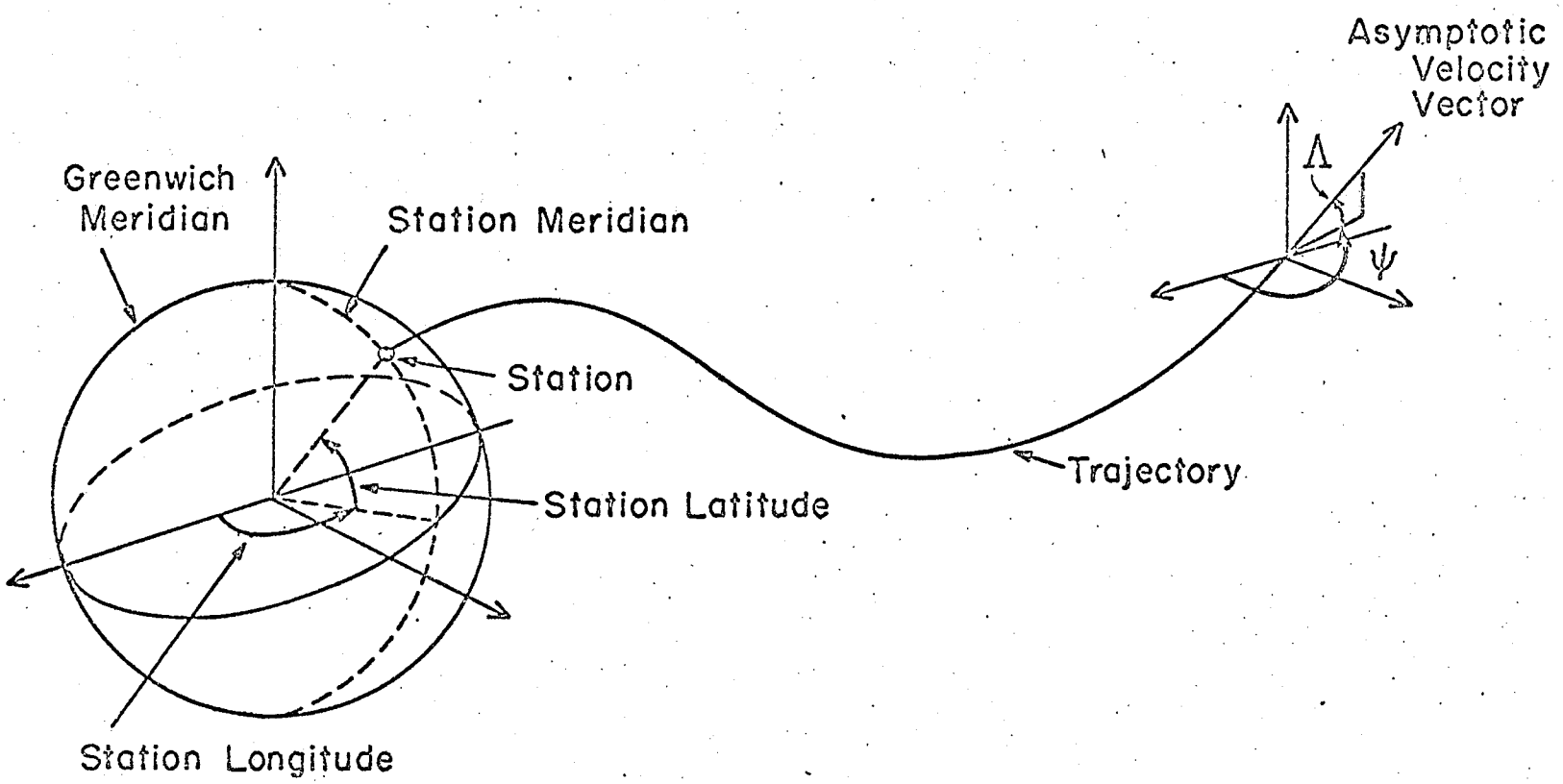
Asymptotic
Velocity
Vector
Λ
ψ
Greenwich
Meridian
Station Meridian
Station
Trajectory
Station Latitude
Station Longitude

IBM 360/65 computer. In this calculation the earth's magnetic field is simulated by the sixth order spherical harmonic expansion of Finch and Leaton (1957). The particle trajectory is traced from an initial point 20 km. above the earth until it either reaches a specified distance of 50 earth radii or its trajectory intersects the earth. In the former case, the particle's final position and velocity are transformed into the required geographic coordinates. Fig. 2.4 shows the dependence of asymptotic viewing direction on primary rigidity corresponding to the axial directions of the two narrow angle inclined telescopes and the megascope.

2.4 Data

The two year period analyzed in this thesis runs from 1530, March 18, 1969 to 2400, March 17, 1971 (local time). The data gathered were transferred from paper tape to computer cards via an I.B.M. model 1620 computer and then stored on a magnetic disc of the IBM 360/65 system. Also stored on disc were local meteorological data and neutron data from Deep River, Ontario. After the collection of the two years of data, all information was permanently stored on magnetic tape in files containing day, hour, telescope rates 12-56 (henceforth called 'A'), 34-56 (henceforth called 'B'), JACK, MIKE, pressure temperature, 24-hour running mean temperature and neutron data. Telescopes JACK and MIKE were summed (henceforth called 'JAMI') for statistical advantages. These data were then handled as shown in Fig. 2.5, to achieve the final results.

If any anomolous deviations occurred due to instability of a

Figure 2.4

Asymptotic directions of approach for Winnipeg muon telescopes. Points marked correspond to primary magnetic rigidities of 19, 30, 45, 70, 95, 150, 450 GeV.

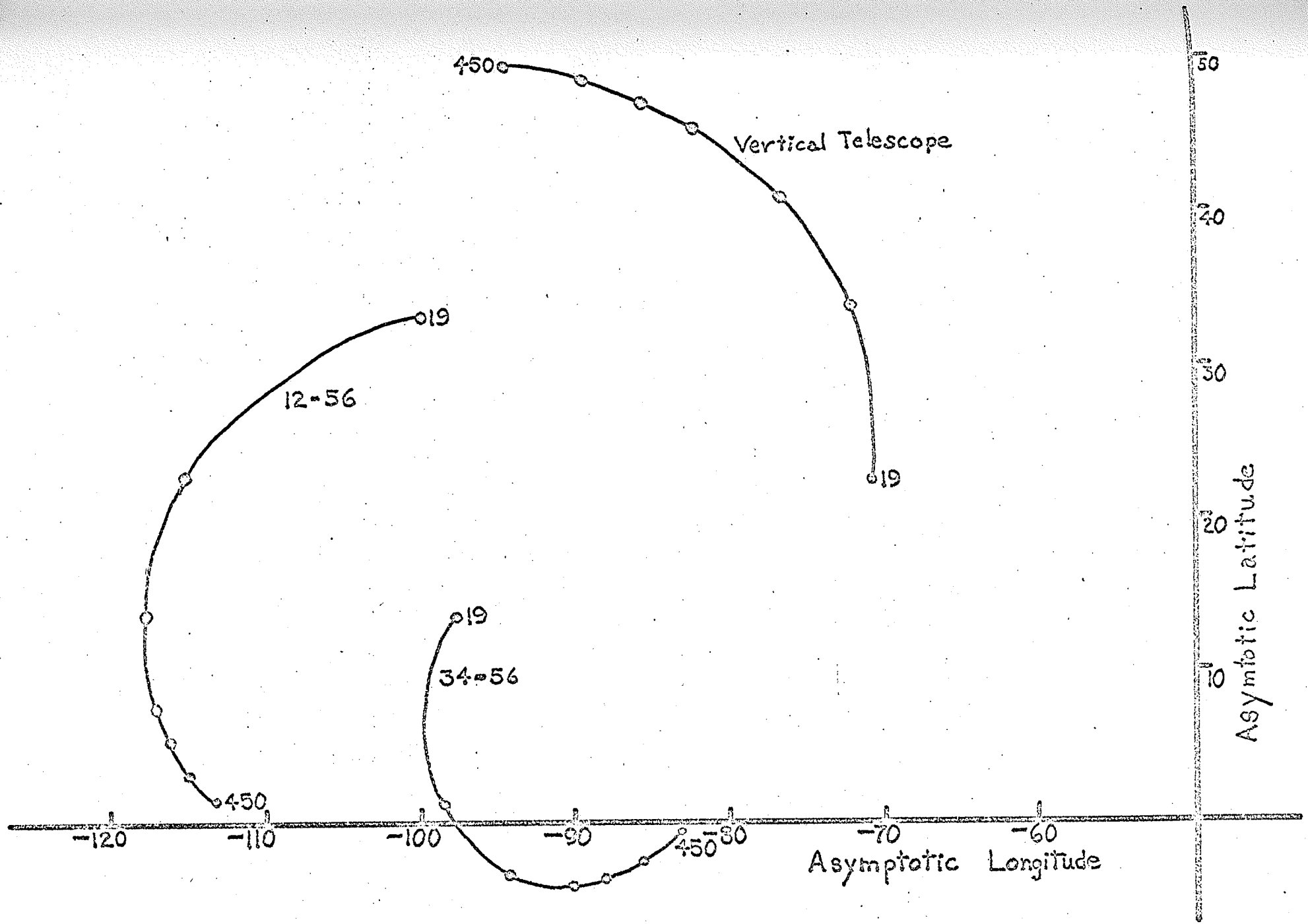
450
Vertical Telescope
19
19
12-56
19
34-56
450
-120
-110
-100
-90
-80
-70
-60
Asymptotic Longitude
50
40
30
20
10
Asymptotic Latitude

Figure 2.5

Schematic representation of procedure adopted for processing the data.

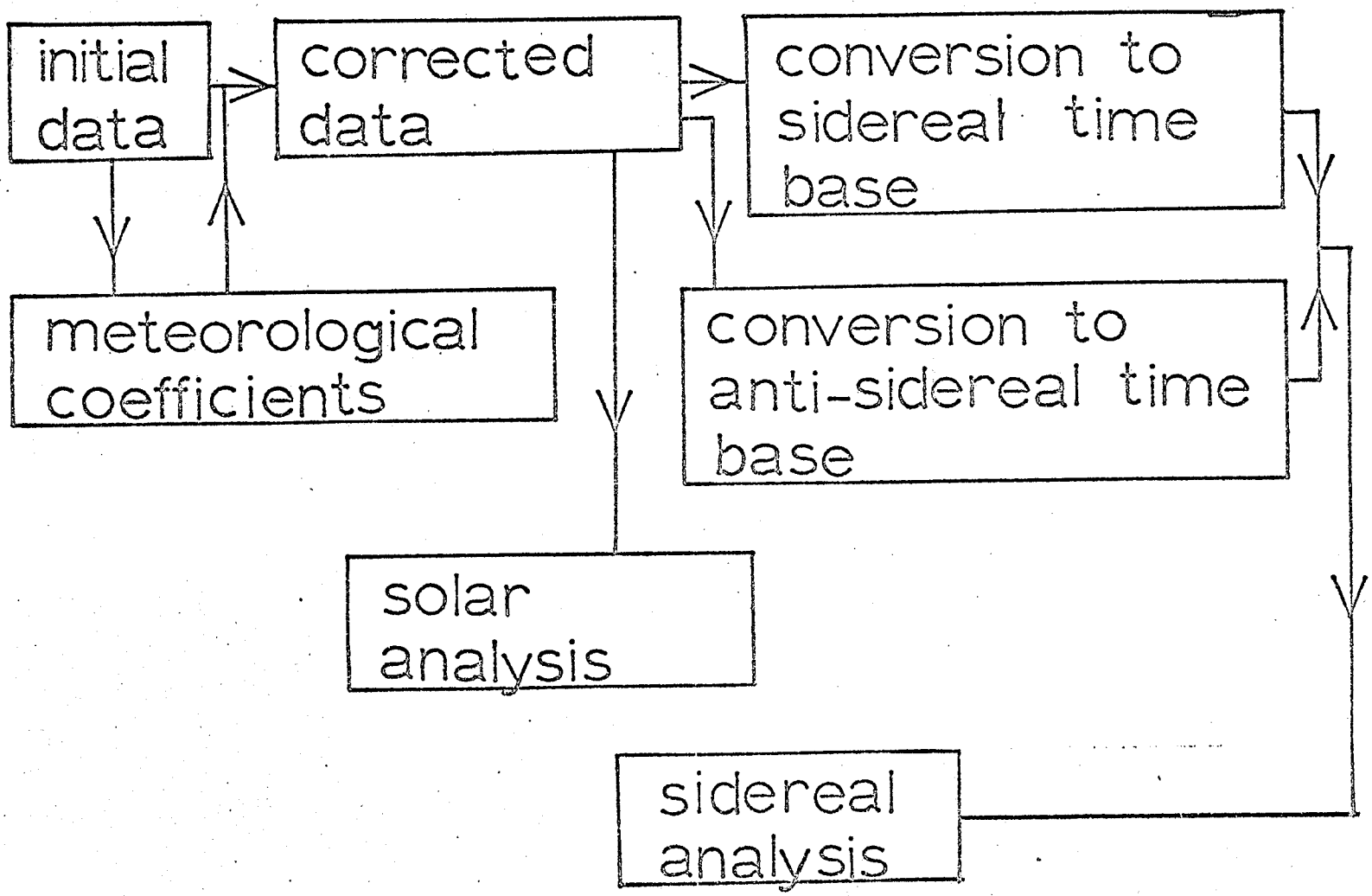
initial data
corrected data
conversion to sidereal time base
meteorological coefficients
conversion to anti-sidereal time base
solar analysis
sidereal analysis

photomultiplier, incorrect readout intervals or any transient instabilities of the apparatus, these points were deleted from the overall survey. Unfortunately, two of the scintillation counters forming the narrow angle verticle telescopes were exposed to uncontrolled influences which resulted in the generation of data which could not be used in this study. Over the two year period, deletions from the remaining telescopes were negligible.

CHAPTER III

CORRECTIONS AND CONVERSIONS

3.1 Meteorological corrections

As previously mentioned, meteorological variations influence cosmic ray intensity. For the detectors under consideration, the predominanting effects are determined by changes in barometric pressure (P) and the atmospheric temperature (T) at the height of the muon production levelin the form

$$\Delta I = C_p \Delta P + C_T \Delta T$$

where ΔI is the change in the intensity and C_p and C_T are the respective coefficients. For an increase in pressure, the atmosphere absorbs more low energy muons before they reach sea level, so that C_p arises from the mass absorption effect. The coefficient C_T, is a result of the competition between the processes of pion-muon decay and nuclear interaction of π -mesons near the production level. Therefore, the observed telescope data must be corrected for these effects before any meaningful conclusions can be reached.

The results of the study undertaken for this thesis (March 18, 1969 to March 17, 1971) will be compared with those obtained by Briggs (1969) who utilized data for the period from November 13, 1966 to May 17, 1968. The determination and application of meteorological correc-

tions will be patterned after his method.

Bercovitch et al. (1963) showed that the pressure corrected meson amplitude on average was proportional to that for the neutron component over a wide range of neutron amplitudes (0 to 1%) so that, although muon and neutron detectors characteristically have their maximum response at different primary energies, the neutron component may be used to represent primary intensity variations as seen by the muon monitor. Also, since the hourly distribution of temperature throughout the atmosphere was not available, it was decided that a 24-hour running mean ground level temperature would represent a closer relation to changes at the height of muon production level than would hourly ground level temperature (the latter was shown by Briggs to be a statistically insignificant parameter). Consequently, regression analyses were applied to the counting rates of both the megascope and the inclined telescopes for quiet periods (i.e. periods free of Forbush decreases with magnitudes $>1\%$), in the manner suggested, to find the coefficients of the appropriate parameters. In both cases, pressure corrected data of a neutron monitor, with a counting rate twice that of the megascope, was obtained from Deep River, Ontario (geographic longitude 77.5° west, geographic latitude 46.1° north). The neutron data were phase shifted to a later time by 1.5 hours in universal time to account for the longitudinal separation of the asymptotic coordinates of the respective monitors.

In the case of the megascope, the muon rate was correlated with three parameters: ground level pressure, P, 24-hour running

mean ground level temperature, T_{24}, and the Deep River neutron monitor rate, N. An expression of the form

$$\Delta I = C_p \Delta P + C_T \Delta T_{24} + C_n \Delta N$$

was used where the prefix Δ represents the deviation of the hourly reading from the mean of the whole period in question. The last term is intended to account for the effect of true primary variation on the muon rate, which as discussed above, is taken to be proportional to the pressure corrected neutron monitor rate. It was found that the coefficients were comparable with those calculated by Briggs. Thus, for the sake of uniformity in the comparison of results, the coefficients used for the meteorological corrections to the megascope were those of Briggs:

$$C_p = (-0.1264 \pm 0.0018) \% / \text{mb}$$

$$C_T = (-0.0797 \pm 0.0023) \% / {}^{\circ}\text{C}.$$

For the inclined telescopes, the method was similar to that for the megascope, with a distinction in that five parameters were used. (For a discussion of the correction procedure see Briggs (1969)).

In addition, to improve statistics on the muon rates, the regression analysis was carried out on a daily mean basis. It was shown by Briggs that such an analysis produces essentially the same meteorological coefficients as an hourly regression analysis. The five parameters were atmospheric pressure, P, long and short term temperatures and long and short term neutron intensities. Long term temperature (and neutron) deviations were defined by

$$\Delta T_L = \bar{T}_{31d} - \bar{\bar{T}}$$

where $\bar{T}_{31d}$ is the 31-day running mean temperature, centred on the day in question, and $\bar{\bar{T}}$ is the average of all such temperatures. Short term temperature (and neutron) deviations are

$$\Delta T_s = \bar{T}_{24h} - \bar{T}_{31d}$$

where $\bar{T}_{24h}$ is the daily mean temperature. The relevant equation for the determination of the coefficients is

$$\Delta I = C_p \Delta P + C_{Ts} \Delta T_s + C_{TL} \Delta T_L + C_{Ns} \Delta N_s + C_{NL} \Delta N_L$$

and again, the coefficients were comparable to those calculated by Briggs so that they too were used for meteorological corrections of the inclined telescopes:

$$C_p = (-0.1593 \pm 0.0056) \ \% / \text{mb}$$

$$C_{Ts} = (-0.106 \pm 0.009) \ \% / {}^{\circ}\text{C}.$$

$$C_{TL} = (-0.919 \pm 0.003) \ \% / {}^{\circ}\text{C}.$$

3.2 Conversion to sidereal and anti-sidereal time bases

For the purpose of seeking sidereal anisotropies, it was necessary to express the meteorological corrected data on a sidereal and an anti-sidereal time base. Since one year (365.25 solar days) consists of 366.25 sidereal days or 364.25 anti-sidereal days (Farley and Storey, 1954), then the largest common integer factor produces

1461 solar records = 1465 sidereal records

= 1457 anti-sidereal records.

Clearly then, sidereal and anti-sidereal records (1 record = 1 hour for the present experiment) are calculated in appropriate cycles as shown diagramatically in Fig. 3.1.

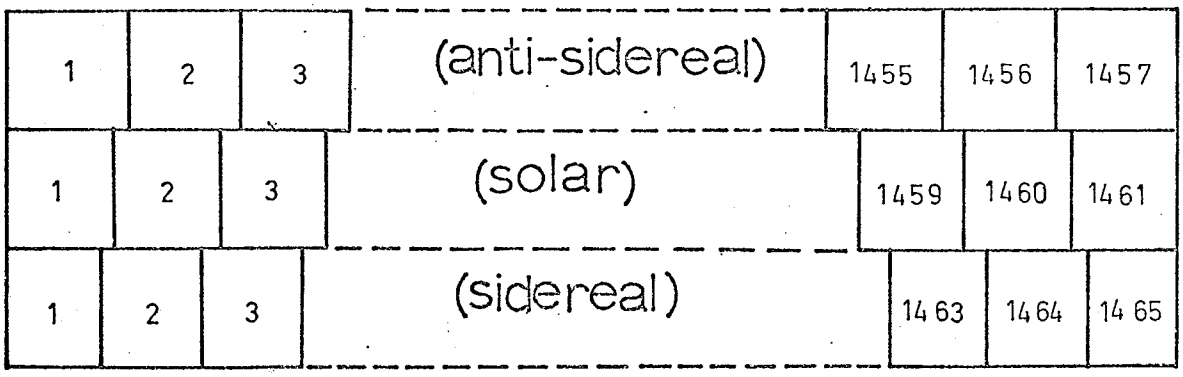

Figure 3.1

Solar, sidereal and anti-sidereal record relationships, on an absolute time scale for one cycle of data conversion.

The two year period of analysis contained 12 such cycles. The conversion formulae are given by Briggs (1969). If any solar record which could not be used in the analysis because of unre-

liable data affected one or more sidereal (anti-sidereal) records, then all such sidereal (anti-sidereal) records were also ignored in further analysis.

CHAPTER IV

SOLAR AND SIDEREAL ANALYSIS

A Fourier analysis was carried out on 24-hour histograms of the hourly percentile deviations from the two year mean for each of the three telescopes (A, B, JAMI). In turn, the data expressed in solar, sidereal and anti-sidereal time bases were analyzed for the amplitudes and phases of the first and second harmonics. The results of these sidereal and anti-sidereal analyses were required in the calculation of a true sidereal result, to be discussed. Solar investigation was carried out for bimonthly segments so as to facilitate a comparison with the results of Briggs (1969). Handling of the true sidereal first harmonics was done in six-month, yearly and biyearly segments for statistical purposes.

For the three telescopes considered, the mean symptotic longitudes applied were those calculated by Briggs (1969a) for an upper energy limit of 100 GeV. utilizing the differential response functions of Krimsky et al. (1966). The mean asymptotic longitude found for the narrow angle vertical telescope was applied to the wide angle vertical telescope (JAMI). The difference between the mean asymptotic longitude and the longitude of the position of the telescope is required to obtain the free-space direction of the Fourier maximum.

4.1 Solar analysis

Daily modulation of the intensity of cosmic rays in solar time gives rise to statistically significant first and second harmonic components. The work of Ables et al. (1966) verified the existence of the semi-diurnal anisotropy. The meteorological corrections were applied to the initial data so as to produce hourly percentile deviations from the average number of counts, over the 730 day period under consideration, for the respective telescopes. Twelve 24-hour histograms of these deviations (consisting of eleven 61-day segments and one 59-day segment numbered consecutively from 1 to 12 commencing on March 18, 1969, to account for the full two year period) were analyzed for the amplitudes and the observed times of the Fourier maxima, then the free space corrections were applied to give the free space times of the maxima. The results of these twelve bimonthly analyses are given in tables 4.1, 4.2 and 4.3 for telescopes A, B and JAMI respectively. These tables present the first and second harmonic components expressing both the observed time of maximum (in hours local time) and the free space time of maximum.

Four figures were constructed to represent these results as a sequential plot of harmonic dial vectors. Fig. 4.1 and Fig. 4.2 show the results of the bimonthly average solar diurnal and semi-diurnal anisotropies, respectively, of telescopes A and B as an extension of those observed by Briggs (1969). The hiatus of 305 days between the last day of Briggs' observations (May 17, 1968) and the first day of the present study (March 18, 1969) is noted by the

open circle containing a dotted line indicating the established trend. The results of the wide angle telescope are shown independently in Fig. 4.3 (diurnal) and Fig. 4.4 (semi-diurnal). The graphs of the solar diurnal anisotropies are plotted on a 24-hour harmonic dial whereas those of the semi-diurnal vectors are done on a 12-hour harmonic dial.

The period considered in this thesis is almost a reflection of that of Briggs about the period of maximum solar activity (see Fig. 4.5). A comparison of the two terms in this light would clearly be of some interest.

Diurnal analyses

From Fig. 4.1 it is clear that the present results indicate a shift to earlier times for the maxima from those established by Briggs, while the amplitudes remain about the same. Fig. 4.3 exhibits the same overall consistency in amplitude with a small irregular oscillation modulating the general observed direction of the vectors. Uncorrelated fine structure in the bimonthly vectors is also present in Fig. 4.1.

The times of maxima over the full two year period are compared with those of Briggs (1969) in Table 4.4. The free space directions of these maxima now occur at slightly earlier times than expected from the azimuthal streaming as proposed by Parker and Axford (i.e. 18.00 hours).

Table 4.1

First and Second Harmonic Components of the Average Daily Intensity Variation of Telescope A

Bimonthly Period	First Harmonic Amplitude %	First Harmonic Observed Time of Maximum (h.L.T.)	First Harmonic Free Space Time of Maximum (h.)	Second Harmonic Amplitude %	Second Harmonic Observed Time of Maximum (h.L.T)	Second Harmonic Free Space Time of Maximum (h.)
1	0.210 ± 0.022	19.4 ± 0.4	18.3 ± 0.4	0.070 ± 0.022	3.9 ± 0.6	2.7 ± 0.6
2	0.139 ± 0.022	18.8 ± 0.6	17.6 ± 0.6	0.065 ± 0.022	4.0 ± 0.6	2.8 ± 0.6
3	0.139 ± 0.022	19.7 ± 0.6	18.6 ± 0.6	0.124 ± 0.022	5.9 ± 0.3	4.5 ± 0.3
4	0.136 ± 0.022	21.7 ± 0.6	20.5 ± 0.6	0.058 ± 0.022	4.6 ± 0.7	3.5 ± 0.7
5	0.140 ± 0.022	19.7 ± 0.6	18.5 ± 0.6	0.099 ± 0.022	3.3 ± 0.4	2.1 ± 0.4
6	0.178 ± 0.022	18.1 ± 0.5	16.9 ± 0.5	0.088 ± 0.022	3.6 ± 0.5	2.4 ± 0.5
7	0.245 ± 0.022	17.9 ± 0.3	16.7 ± 0.3	0.039 ± 0.020	8.0 ± 1.1	1.9 ± 1.1
8	0.189 ± 0.022	19.1 ± 0.4	17.9 ± 0.4	0.057 ± 0.022	4.5 ± 0.7	3.3 ± 0.7
9	0.090 ± 0.022	17.3 ± 0.9	16.1 ± 0.9	0.087 ± 0.022	5.2 ± 0.5	4.1 ± 0.5
10	0.160 ± 0.022	16.1 ± 0.5	14.9 ± 0.5	0.083 ± 0.022	1.9 ± 0.5	0.8 ± 0.5
11	0.159 ± 0.022	17.2 ± 0.5	16.0 ± 0.5	0.083 ± 0.022	3.5 ± 0.5	2.3 ± 0.5
12	0.218 ± 0.022	17.3 ± 0.4	16.4 ± 0.4	0.099 ± 0.022	3.2 ± 0.4	2.1 ± 0.4
full year period	0.154 ± 0.006	18.5 ± 0.2	17.3 ± 0.2	0.067 ± 0.006	3.9 ± 0.4	2.8 ± 0.4

Table 4.2

First and Second Harmonic Components of the Average Daily Intensity Variations of Telescope B

Bimonthly Period	First Harmonic Amplitude %	First Harmonic Observed Time of Maximum (h.L.T.)	First Harmonic Free Space Time of Maximum (h.)	Second Harmonic Amplitude %	Second Harmonic Observed Time of Maximum (h.L.T.)	Second Harmonic Free Space Time of Maximum (h.)
1	0.372 ± 0.022	16.8 ± 0.2	17.2 ± 0.2	0.199 ± 0.022	3.6 ± 0.2	4.0 ± 0.2
2	0.154 ± 0.022	18.0 ± 0.5	18.3 ± 0.5	0.092 ± 0.022	0.6 ± 0.5	1.0 ± 0.5
3	0.118 ± 0.022	16.9 ± 0.7	17.3 ± 0.7	0.053 ± 0.022	3.7 ± 0.8	4.1 ± 0.8
4	0.050 ± 0.022	18.2 ± 1.7	18.6 ± 1.7	0.053 ± 0.022	2.3 ± 0.8	2.7 ± 0.8
5	0.195 ± 0.022	17.4 ± 0.4	17.8 ± 0.4	0.164 ± 0.022	1.8 ± 0.3	2.2 ± 0.3
6	0.186 ± 0.022	16.3 ± 0.5	16.7 ± 0.5	0.061 ± 0.022	1.9 ± 0.7	2.3 ± 0.7
7	0.226 ± 0.022	15.8 ± 0.4	16.2 ± 0.4	0.095 ± 0.022	1.2 ± 0.4	1.6 ± 0.4
8	0.186 ± 0.022	16.8 ± 0.5	17.1 ± 0.5	0.076 ± 0.022	2.6 ± 0.6	3.0 ± 0.6
9	0.144 ± 0.022	14.7 ± 0.6	15.1 ± 0.6	0.105 ± 0.022	2.4 ± 0.4	2.8 ± 0.4
10	0.161 ± 0.022	15.2 ± 0.5	15.6 ± 0.5	0.101 ± 0.022	1.7 ± 0.4	2.0 ± 0.4
11	0.238 ± 0.022	16.1 ± 0.4	16.5 ± 0.4	0.132 ± 0.022	2.2 ± 0.3	2.6 ± 0.3
12	0.271 ± 0.022	16.4 ± 0.3	16.8 ± 0.3	0.137 ± 0.022	1.9 ± 0.3	2.4 ± 0.3
full two year period	0.184 ± 0.006	16.4 ± 0.1	16.8 ± 0.1	0.095 ± 0.006	2.2 ± 0.3	2.6 ± 0.3

Table 4.3

First and Second Harmonic Components of the Average Daily Intensity Variation of Telescope JAMI

	First Harmonic			Second Harmonic		
Bimonthly Period	Amplitude %	Observed Time of Maximum (h.L.T.)	Free Space Time of Maximum (h.)	Amplitude %	Observed Time of Maximum (h.L.T.)	Free Space Time of Maximum (h.)
1	0.218 ± 0.004	15.9 ± 0.1	17.3 ± 0.1	0.044 ± 0.004	2.2 ± 0.2	3.6 ± 0.2
2	0.186 ± 0.004	15.6 ± 0.1	16.9 ± 0.1	0.033 ± 0.004	2.3 ± 0.2	2.6 ± 0.2
3	0.147 ± 0.004	17.4 ± 0.1	18.7 ± 0.1	0.020 ± 0.004	4.5 ± 0.3	5.9 ± 0.3
4	0.146 ± 0.004	14.3 ± 0.1	15.7 ± 0.1	0.050 ± 0.004	1.4 ± 0.1	2.8 ± 0.1
5	0.137 ± 0.004	13.7 ± 0.1	15.1 ± 0.1	0.057 ± 0.004	1.1 ± 0.1	2.4 ± 0.1
6	0.087 ± 0.004	14.5 ± 0.2	15.9 ± 0.2	0.006 ± 0.004	2.6 ± 1.2	4.0 ± 1.2
7	0.153 ± 0.004	15.9 ± 0.1	17.3 ± 0.1	0.039 ± 0.004	3.2 ± 0.2	4.5 ± 0.2
8	0.306 ± 0.004	15.6 ± 0.04	17.0 ± 0.04	0.022 ± 0.004	0.40 ± 0.3	1.7 ± 0.3
9	0.169 ± 0.004	15.8 ± 0.1	17.1 ± 0.1	0.028 ± 0.004	1.8 ± 0.2	3.1 ± 0.2
10	0.184 ± 0.004	15.7 ± 0.1	17.0 ± 0.1	0.028 ± 0.004	11.3 ± 0.2	0.7 ± 0.2
11	0.193 ± 0.004	13.9 ± 0.1	15.3 ± 0.1	0.053 ± 0.004	1.1 ± 0.1	2.5 ± 0.1
12	0.200 ± 0.004	13.9 ± 0.1	15.2 ± 0.1	0.049 ± 0.004	0.6 ± 0.2	2.0 ± 0.2
full two year period	0.170 ± 0.001	15.3 ± 0.02	16.7 ± 0.02	0.030 ± 0.001	1.6 ± 0.1	2.9 ± 0.1

Figure 4.1

Sequential plots of bimonthly average solar diurnal anisotropy vectors for telescopes A and B, on a 24-hour harmonic dial for period November 13, 1966 to March 17, 1971. Open circle represents a 305 day hiatus in the sequence.

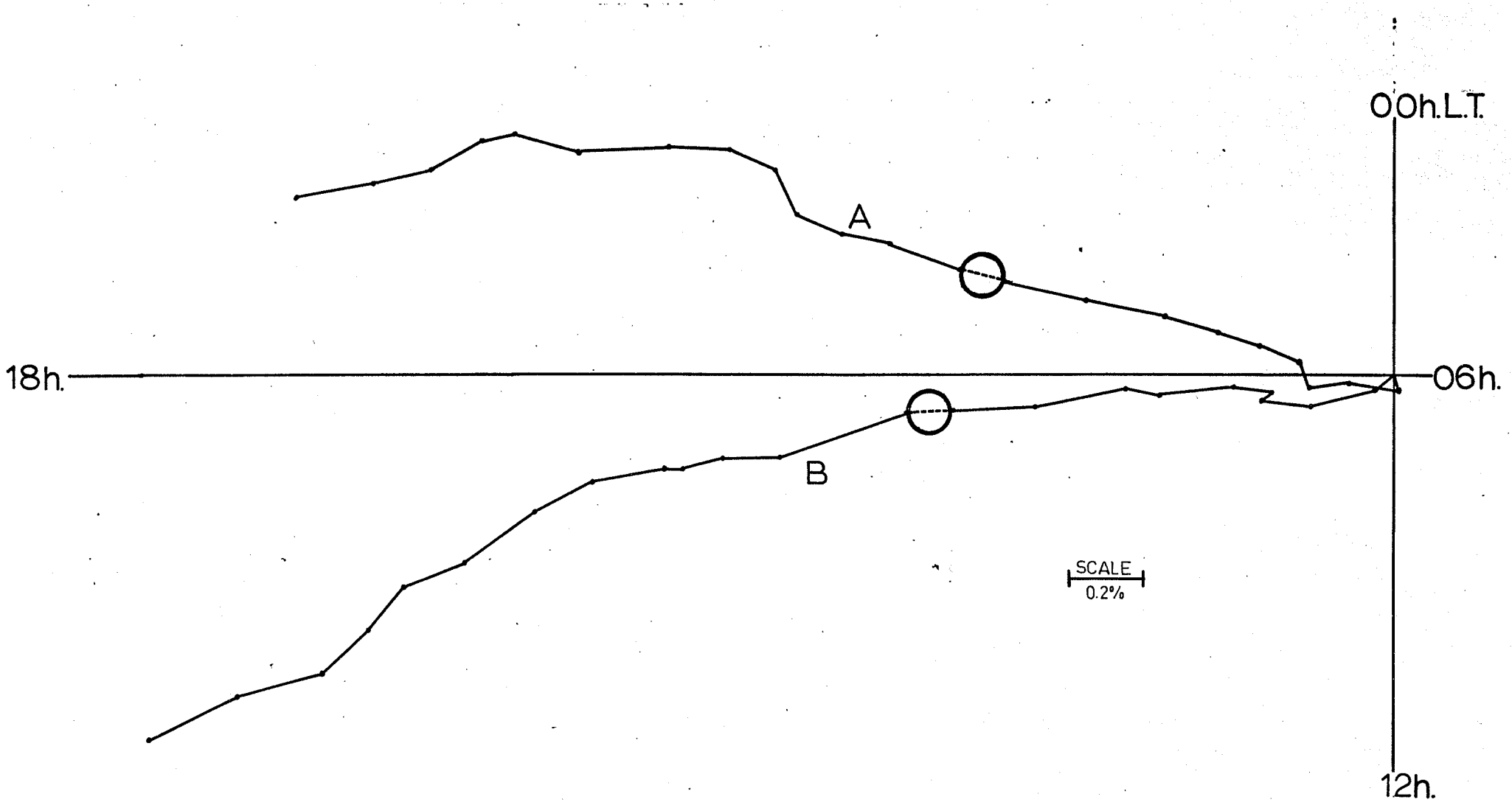
00h.L.T.
A
18h.
06h.
B
SCALE
0.2%
12h.

Figure 4.2

Sequential plot of bimonthly average solar semi-diurnal anisotropy vectors for telescopes A and B, on a 12-hour harmonic dial for period November 13, 1966 to March 17, 1971. Open circle represents a 305 day hiatus in the sequence.

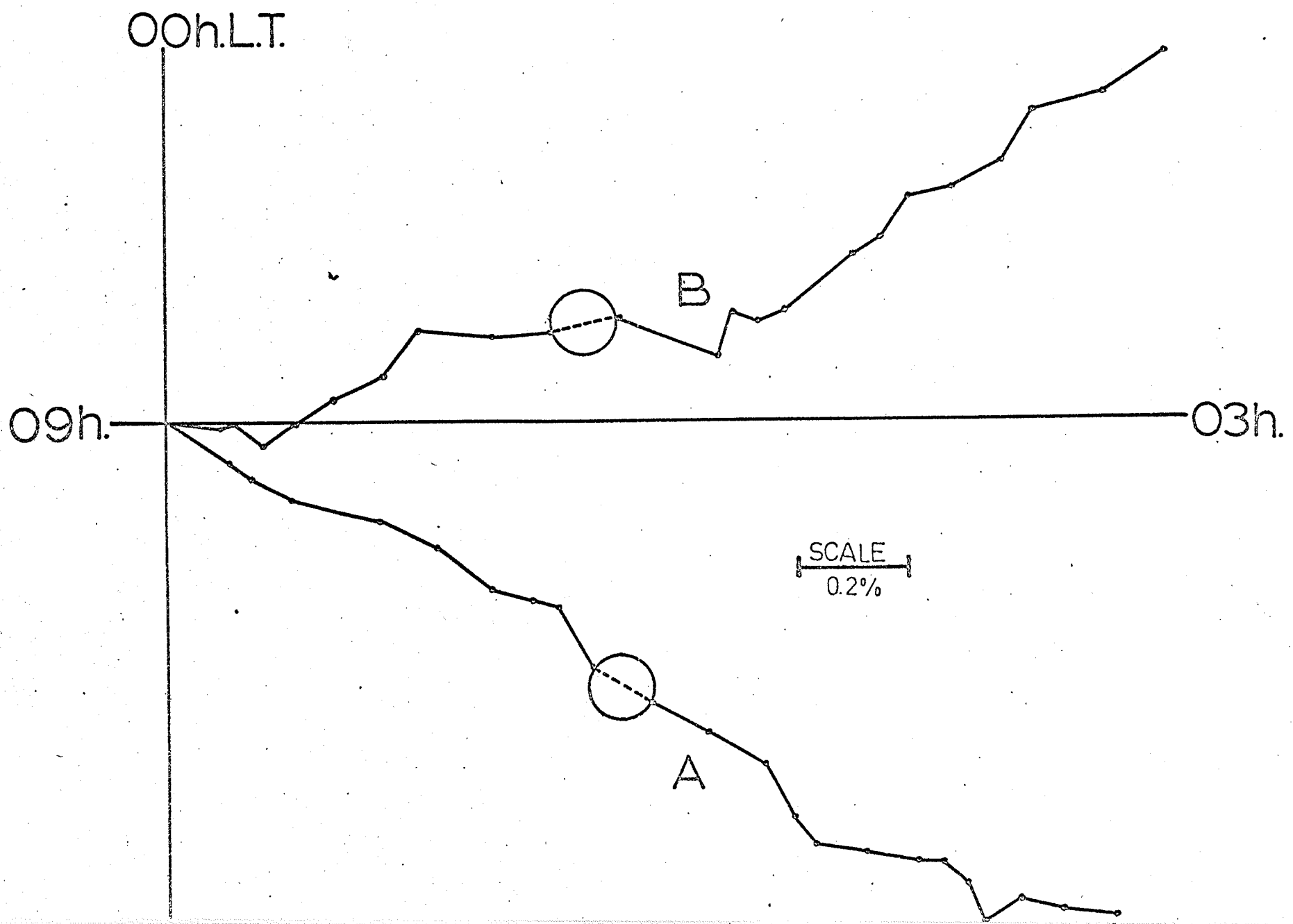
00h.L.T.
09h.
03h.
B
A
SCALE
0.2%

Figure 4.3

Sequential plot of bimonthly average solar diurnal anisotopy vectors for telescope JAMI, on a 24-hour harmonic dial.

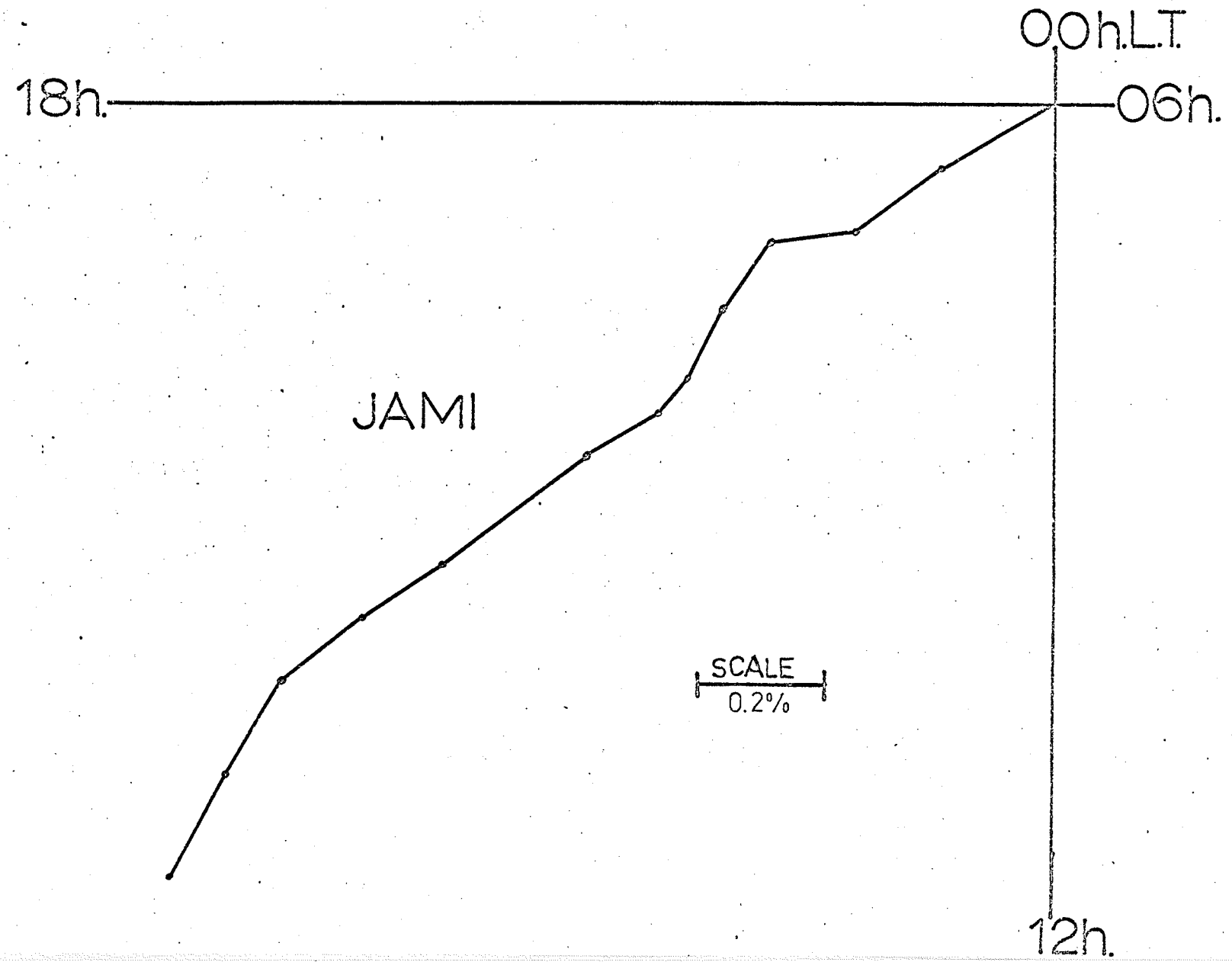
00h.L.T.
18h.
06h.
JAMI
SCALE
0.2%
12h.

Figure 4.4

Sequential plot of bimonthly average solar semi-diurnal anisotropy vectors for telescope JAM, on a 12-hour harmonic dial.

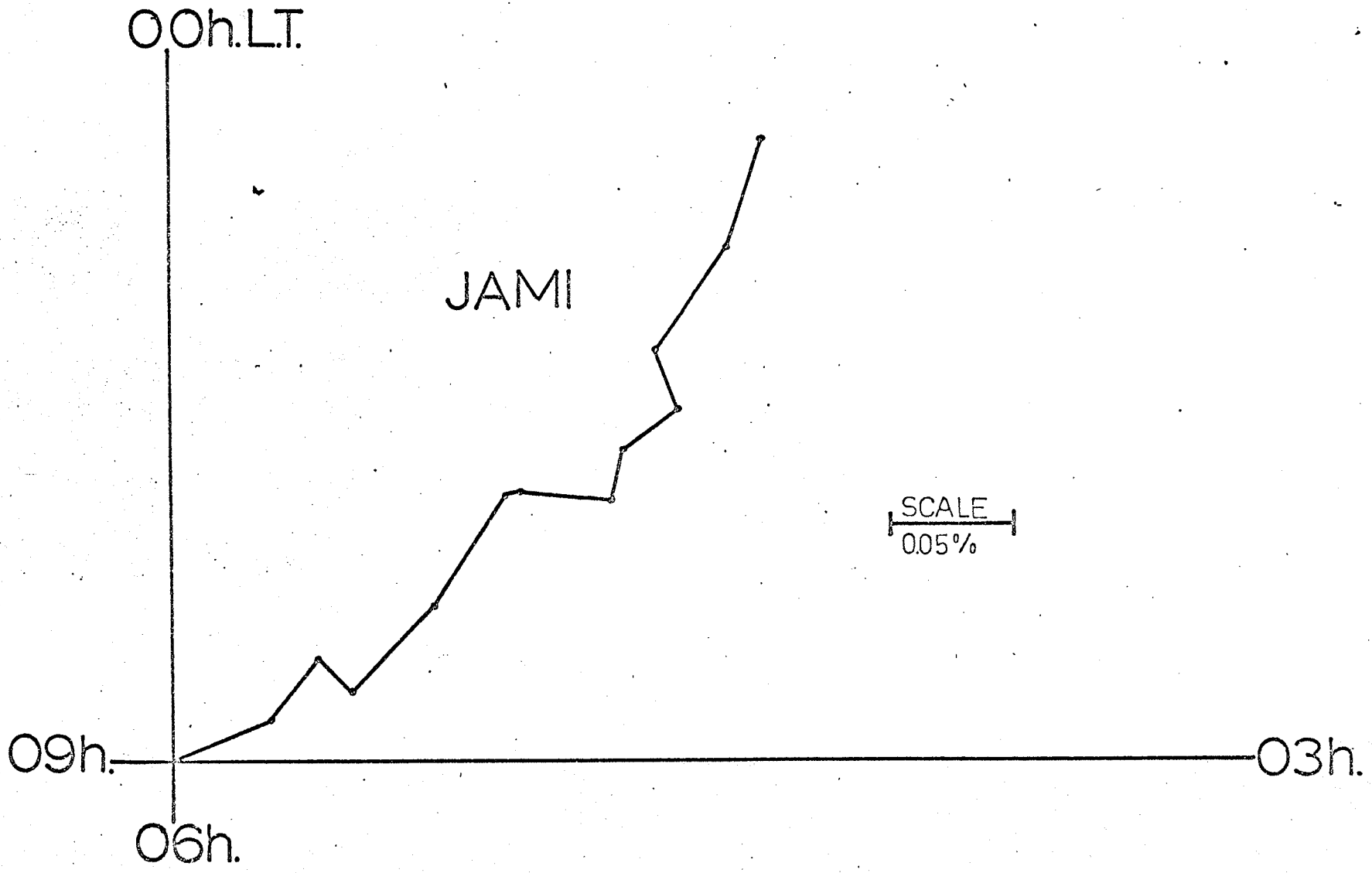
00h.L.T.
JAMI
SCALE
0.05%
09h.
03h.
06h.

Figure 4.5

Eleven year sunspot cycle indicating periods considered by Briggs (1969) and the present study.

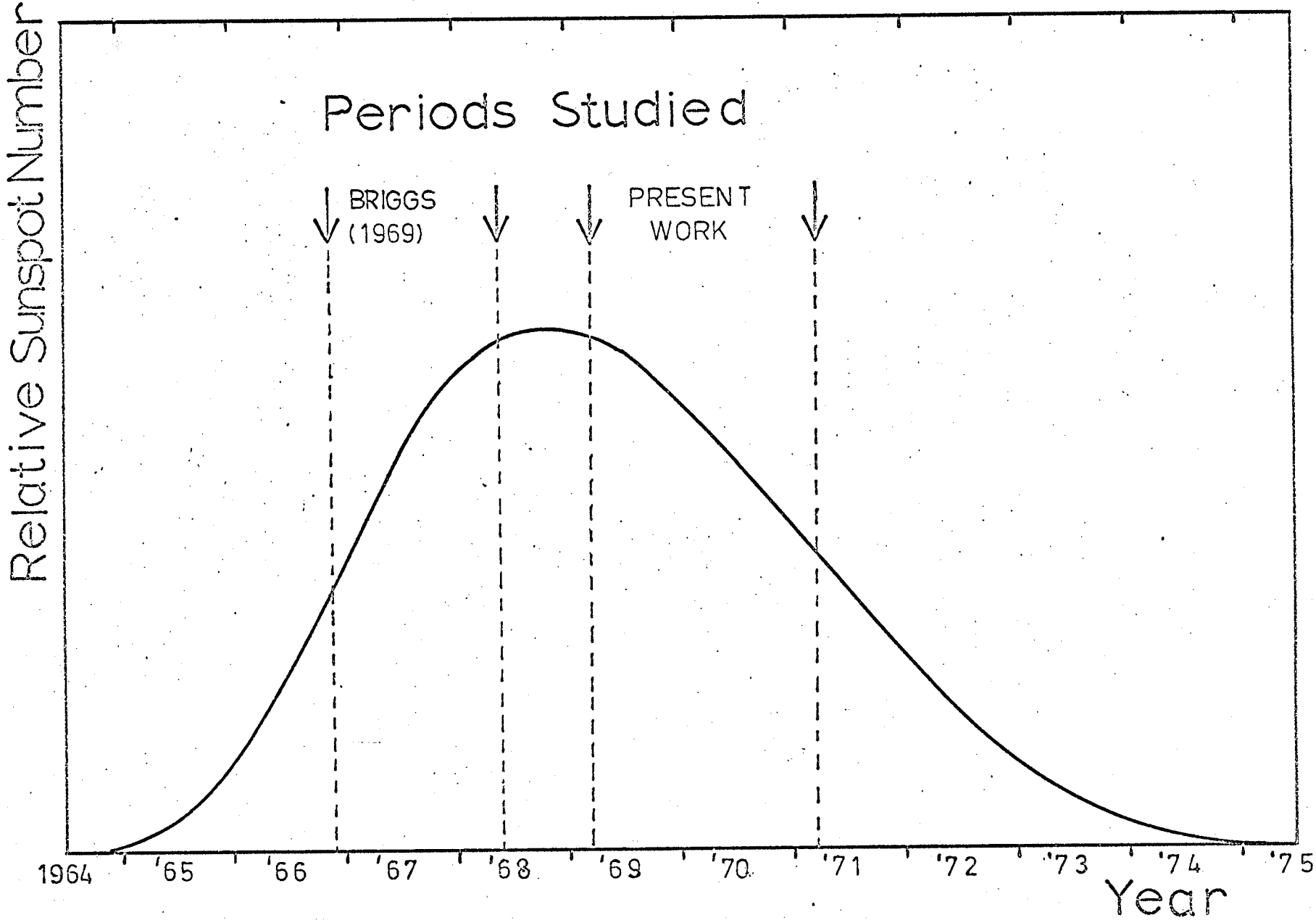
Periods Studied
BRIGGS
(1969)
PRESENT
WORK
Relative Sunspot Number
1964
'65
'66
'67
'68
'69
'70
'71
'72
'73
'74
'75
Year

Table 4.4

Times of maxima of first harmonic observed by Briggs and present study

	Observed time of maximum (h.L.T.)	Free space time of maximum (hours)
Telescope A:		
(Present result)	18.47 ± 0.16	17.31 ± 0.16
(Briggs)	18.97 ± 0.38	17.80 ± 0.38
Telescope B:		
(Present result)	16.41 ± 0.13	16.80 ± 0.13
(Briggs)	17.88 ± 0.40	18.28 ± 0.40
Telescope JAN:		
(Present result)	15.31 ± 0.02	16.65 ± 0.02

The present results suggest a small change of phase in this later part of the solar cycle, possibly attributed to different interplanetary conditions impressed upon the azimuthal streaming mechanism.

Semi-diurnal analyses

The bimonthly average solar semi-diurnal anisotropy vectors for telescopes A and B plotted in Fig. 4.2 again exhibit amplitudes comparable to those of Briggs and again, the present results indicate a shift to earlier times for the maxima from that established by Briggs. The amplitudes appear to be slightly more steady for Telescope A than those of Telecope B which show an increasing trend for the last four bimonthly periods. Table 4.5 compares the times of

maximum (observed local time and free space time) for the entire period under consideration in this survey with those observed by Briggs.

Table 4.5

Times of maxima of second harmonic observed by Briggs and present study

	Observed time of maximum (h.L.T.)	Free space time of maximum (hours)
Telescope A:		
(present study)	3.93 ± 0.36	2.77 ± 0.36
(Briggs)	4.11 ± 0.47	2.95 ± 0.47
Telescope B:		
(present study)	2.20 ± 0.25	2.59 ± 0.25
(Briggs)	2.60 ± 0.60	3.00 ± 0.60
Telescope JAMI:		
(Present study)	1.57 ± 0.07	2,91 ± 0.07

The free space directions for the present study shown in Table 4.5 correspond to 138.45 ± 5.40°, 141.50 ± 3.75° and 136.35 ± 1.05° west of the earth-sun line and 41.55 ± 5.40°, 38.85 ± 3.75° and 43.65 ± 1.05° east of the earth-sun line for telescopes A, B and JAMI respectively. As with the diurnal anisotropies, these figures appear at slightly esrlier times than expected from the Lietti and Quenby (1966) for the semi-diurnal anisotropy (i.e. 3.00 hours free space time or 135° west and 45° east of the earth sun line). This, again, suggests a dependence upon the period of solar cycle under consideration.

4.2 Sidereal analyses

The average daily variation of the data was computed on a sidereal time base. However, since the solar daily variation is not constant in time and periods of less than twelve months were analyzed, fictitious anisotropies appear in the average sidereal daily variations. These spurious variations may be eliminated assuming:

i) the first harmonic of the solar anisotropy is amplitude-modulated only (i.e. constant in phase)

ii) the sidereal anisotropy is constant in time

iii) any sidereal anisotropy is small compared to the solar anisotropy

To do the standard sidereal analysis (Briggs 1969) the following procedures were carried out:

A 24 - hour histogram was established for each of the solar, sidereal and anti-sidereal daily variations, which was then Fourier analyzed. The antisidereal curve was reflected about the time of maximum of the solar first harmonic, and this reflected curve then subtracted from the sidereal curve. The resulting difference curve represents the sidereal average daily variation corrected for any spurious variation due to amplitude modulation of the solar first harmonic. However, this method is approximate since none of the assumptions (i) to (iii) is completely justifiable. This method was applied to the semi-yearly, yearly and biyearly blocks to produce the sidereal results listed in Table 4.4.

Table 4.4

Sidereal First Harmonic Components

	Telescope A		Telescope B		Telescope JAM	
Months	Amplitude %	Time of Maximum (h.L.T.)	Amplitude %	Time of Maximum (h.L.T.)	Amplitude %	Time of Maximum (h.L.T.)
1 - 6	0.053 ± 0.021	22.4 ± 1.6	0.291 ± 0.022	7.1 ± 0.3	0.024 ± 0.004	17.8 ± 0.6
7 - 12	0.100 ± 0.020	14.0 ± 0.8	0.276 ± 0.024	14.0 ± 0.3	0.025 ± 0.003	20.0 ± 0.5
13 - 18	0.008 ± 0.025	23.5 ± 11.7	0.172 ± 0.024	6.1 ± 0.5	0.057 ± 0.004	19.6 ± 0.3
19 - 24	0.046 ± 0.026	21.0 ± 2.1	0.311 ± 0.027	19.1 ± 0.3	0.050 ± 0.004	2.4 ± 0.3
1 - 12	0.043 ± 0.015	16.4 ± 1.3	0.176 ± 0.027	10.4 ± 0.4	0.048 ± 0.003	0.8 ± 0.2
13 - 24	0.036 ± 0.018	2.3 ± 1.9	0.077 ± 0.018	20.1 ± 0.9	0.054 ± 0.003	1.8 ± 0.2
1 - 24	0.005 ± 0.011	17.6 ± 8.2	0.056 ± 0.012	11.8 ± 0.8	0.051 ± 0.002	1.3 ± 0.1

The amplitudes of the sidereal first harmonics vary from values near zero to those comparable with the results of Jacklyn (1965) (0.045 ± 0.003 at 6.1 ± 0.25 hours local sidereal time), Peacock et al. (1968) (0.03 ± 0.01 at 18 to 20 hours local sidereal time) and Sekido et al. (1968) (0.054 ± 0.017 at 18.5 ± 0.2 hours right ascension) to amplitudes significantly larger than these, by almost an order of magnitude. In addition to this, the times of maxima are very widely scattered.

Because of the very liberal assumptions utilized in locating and measuring sidereal anisotropies, the results of the analysis are questionable. This, combined with the inconsistent amplitudes and phases of the sidereal results, indicates the results are highly suspect. The phase of the solar first harmonic, which is only roughly constant in the bimonthly averages, will be considerably less constant on a day to day basis. Nor is the solar anisotropy large compared with these of the sidereal in every instance. The assumptions on which the analysis was based are clearly untenable and thus the results are not significant.

4.3 Conclusions

This survey for the period March 18, 1969 to March 17, 1971 has extended the work of Briggs (November 13, 1966 to May 17, 1968) and basically confirmed his results:

(i) The free space times of maximum of the first harmonic intensity variations were found to be in agreement with the co-rotational theories of Parker and Axford. The mean amplitude of the first harmonic effect for the narrow angle telescopes was 0.17%.

(ii) A second harmonic of mean amplitude 0.08% was found with free space times of maxima at 2.7 h and 14.7 h.

In addition it has indicated small phase changes to earlier times, probably related to changing interplanetary conditions throughout the solar cycle. The analysis for sidereal anisotropies is inconclusive.

BIBLIOGRAPHY

Ables, J. G., McCracken, K. G. and Rao, M. R., Proc, 9th Int. Conf. Cosmic Rays, (London) 1, 208 (1966).

Axford, W. I., Planet. Space Sci., 13, 115 (1965).

Bercovitch, M., Steljes, J. F. and Carmichael, H., Proc. 8th Int. Conf. Cosmic Rays (Jaipur), 2, 327 (1963).

Blackett, P. M. S. and Occhialini, G. P. S., Proc. Roy. Soc. (London), A139, 699 (1933).

Bothe, W. and Kolhorster, W., Naturwiss, 16, 1044, 1045 (1928).

Bothe, W. and Kolhorster, W., Phys, Zeits., 30, 516 (1929).

Briggs, M. M., M. Sc. Thesis Univ. of Manitoba, Canada (1965).

Briggs, R. M. and Standil, S., Bull. Am. Phys. Soc., 11, 470 (1966).

Briggs, M. M., Ph. D. Thesis Univ. of Manitoba, Canada (1969).

Briggs, R. M., Hicks, R. B. and Standil, S., J. Phys., A 2, 584 (1969).

Carmichael, H., Bercovitch, M. and Steljes, J. F., Proc, 9th Int Conf. Cosmic Rays (London), 1, 492, (1966).

Carmichael, H., Bercovitch, M. and Steljes, J. F., Tellus, 19, 143, (1967).

Clay, J., Proc. Amsterdam, 30, 1115 (1927).

Compton, A. H., Bennett, R. D. and Stearns, J. C., Phys, Rev., 41, 119 (1932).

Elster, J., Phys, Zeits., 2, 506 (1900).

Farley, F. J. M. and Storey, J. R., Proc., Phys. Soc. A, 67, 996 (1954).

Finch, H. F. and Leaton, B. R., Monthly Notices Roy Astron Soc., Geophys. Suppl., 1, 314 (1957).

Geftel, M., Phys. Zeits., 2, 116 (1900).

Hess, V. F., Phys. Zeits., 12, 998 (1911).

Hess, V. F., Phys. Zeits., 13, 1084 (1912).

Hess, V. F., and Graziadei, M. T., Terr. Mag. Atm. Elect., 41, 9 (1936).

Jacklyn, R. M., Nuovo Cim., 36, 1135 (1965).

Johnson, T. H., Phys. Rev., 43, 307, 381 (1933).

Kolhorster, W., Phys. Zeits., 14, 307, 1153 (1913).

Krimsky, G. F., Krivoshapkin, P. A. and Skripin, G. V., Proc. 9th Int. Conf. Cosmic Rays, (London) 1, 503 (1966).

Lange, I. and Forbush, S. E., Carnegie Inst. of Wash. Publ. 175 (1948).

Lietti, B. and Quenby, J.J., Can. J. Phys., 46, S942 (1968).

Lindholm, F., Gerl. Beitr. Geophys., 20, 12 (1928).

McCracken, K. G., Rao, U. R. and Shea, M. A., M.I.T. Tech. Report No. 77 (1962).

Mercer, J. B. and Wilson, B. G., Nature, 208, 477 (1965).

Parker, E. N., Planet. Space Sci., 12, 735 (1964).

Parker, E. N., Planet. Space Sci., 15, 1723 (1967).

Parker, E. N., Interplanetary Dynamical Processes, Interscience Publ., John Wiley and Sons.

Patel, D., Sarabhai, V. and Subramanian, G., Planet. Space Sci., 16, 1131 (1968).

Peacock, D. S., Dutt, J. C. and Thambyahpillai, T., Can. J. Phys., 46, S788, (1968).

Rossi, B., Nature, 125, 636 (1930a).

Rossi, B., Lincei Rend., 11, 831 (1930b).

Rossi, B., Ric. Sci., 5, 569 (1934).

Rossi, B., Rev. Mod.Phys., 20, 537 (1948).

Sarabhai V. and Subramanian, G., Astrophys. J., 145, 206 (1966).

Schonland, B. F. J., Delatizly, B. and Gaskell, J., Terr. Mag. Atm. Elect., 42, 137 (1937).

Sekido, Y., Nagashima, K., Kondo, I., Murayama, T., Okunda, H., Sakakibara, S. and Fujimoto, K., Can. J.Phys., 46, S607 (1968).

Skobeltzyn, D. V., Z. Physik, 43, 354 (1927).

Subramanian, G. and Sarabhai, Astrophys. J., 149, 417 (1967).

Swinson, D. B., J. Geophys. Res., 74, 5591 (1969).

Swinson, D. B., J. Geophys. Res., 75, 7303 (1970).

Swinson, D. B., J. Geophys. Res., 76, 4217 (1971).

Waddington, C. J., Prog. Nucl. Phys., 8, 1 (1960).

Wilson, C. T. R., Proc. Camb. Phil. Soc., 11, 521 (1900).

Wilson, C. T. R., Proc. Roy. Soc. (London), A68, 151; A69, 277 (1901).